

**THE ROCKETDYNE MULTIFUNCTION TESTER -
PART II: OPERATION OF A RADIAL MAGNETIC BEARING AS AN EXCITATION SOURCE***

L.A. Hawkins, B.T. Murphy, and K.W. Lang
Rockwell International
Canoga Park, California 91304, U.S.A.

The operation of the magnetic bearing used as an excitation source in the Rocketdyne Multifunction Tester is described. The tester is scheduled for operation during the summer of 1990. The magnetic bearing can be used in two control modes: 1) open loop mode, in which the magnetic bearing operates as a force actuator, and 2) closed loop mode, in which the magnetic bearing provides shaft support. Either control mode can be used to excite the shaft; however, response of the shaft in the two control modes is different due to the alteration of the eigenvalues by closed loop mode operation. A rotordynamic model is developed to predict the frequency response of the tester due to excitation in either control mode. Closed loop mode excitation is shown to be similar to the excitation produced by a rotating eccentricity in a conventional bearing. Predicted frequency response of the tester in the two control modes is compared, and the maximum response is shown to be the same for the two control modes when synchronous unbalance loading is not considered. The analysis shows that the response of this tester is adequate for the extraction of rotordynamic stiffness, damping, and inertia coefficients over a wide range of test article stiffnesses.

INTRODUCTION

Active magnetic bearings have been developed by numerous researchers for an increasing number of tasks. Schweitzer and Lange (ref. 1), Stanway and Burrows (ref. 2), and Salm and Schweitzer (ref. 3) have described strategies for using magnetic bearings to actively control the motion of a flexible rotor. Nikolajsen (ref. 4), Allaire (ref. 5), and Kasarda (ref. 6) have described the use of magnetic bearings as damping devices. The first commercially available magnetic bearing was introduced by Societe Europeenne de Propulsion/Societe de Mecanique Magnetique (SEP/S2M) of France in the early 1980s. Industrial applications of these bearings as primary bearings in rotating machinery have been described by Foster (ref. 7), Weise (ref. 8), and Brunet (ref. 9). Habermann and Brunet (ref. 10), Weise (ref. 11), Humphris (ref. 12), and Chen and Darlow (ref. 13) have presented details of practical magnetic bearing control systems. Chen (ref. 14) translated the parameters of a magnetic bearing control system into stiffness and damping coefficients for use in a rotordynamic analysis.

A radial magnetic bearing is used in the Rocketdyne Multifunction Tester (RMT) as

*This work was funded by AFAL Contract F04611-86-C-0103 (Program Monitor, Al Kudlach).

an excitation source for the identification of rotordynamic coefficients (ref. 15). The use of a magnetic bearing as an excitation source has been described by Ulbrich (ref. 16) and Wagner and Pietruszka (ref. 17). Wagner and Pietruszka used the magnetic bearing as a known force input device for the identification of rotordynamic coefficients in a test stand. In the RMT, the magnetic bearing is used as a motion input device, and test article reaction force is determined independently through a calibrated backup spring. The backup spring, or flex mount, has a stiffness of $5.25E+8$ N/m ($3.0 E+6$ lb/in) and is instrumented with accelerometers and high resolution displacement probes. As an excitation source, the magnetic bearing must meet two requirements: 1) provide a shaft displacement at the test article of $1.25E-5$ m (0.5 mils) minimum, and 2) provide a deflection of the flex mount of $1.25E-6$ m (50 μ in) minimum. These two requirements are necessary to provide adequate accuracy for the calculation of the rotordynamic coefficients. These requirements must be met over a large portion of the 0 - 400 Hz excitation range. The primary motivation for the study described here was to determine if the magnetic bearing would produce the necessary response at the test article.

The magnetic bearing used in the RMT can be used to excite the shaft in either of two control modes - closed loop or open loop. The response of the tester will be different in the two control modes; therefore, response to the two control modes is compared to determine which control mode produces the better response. Open loop excitation can be treated simply by applying a forcing function directly to the shaft (ref. 17). The authors are not aware of a published analysis of the magnetic bearing as an excitation source in closed loop mode. An analysis is presented here that shows closed loop excitation of a rotor to be analogous to a rotating eccentricity at a conventional bearing. The analysis is then used to predict the maximum frequency response of the RMT rotor to magnetic bearing excitation.

RADIAL MAGNETIC BEARING

A schematic for a simple magnetic bearing is shown in Figure 1. The magnetic force developed in the air gap of the magnetic bearing is given by

$$F = \mu A_p N^2 i^2 / 2h^2. \quad (1)$$

Since only the current, i , and the gap clearance, h , can change, this leads to the relation

$$\Delta F = -K_i \Delta i - K_y \Delta y \quad (2)$$

where for two pairs of magnetic poles, K_i and K_y are given by Kasarda (ref. 6) as

$$K_i = -(4\mu_0 A_p N^2 i_s) / (h_s^2) \quad (3)$$

$$K_y = -(4\mu_0 A_p N^2 i_s^2) / (h_s^3) \quad (4)$$

The current stiffness, K_i , is negative, indicating that an increase in current forces the mass away from its equilibrium position (toward the magnet), (ref. 12). The position stiffness, K_y , is also negative, indicating that a positive displacement toward the magnet forces the mass further from its equilibrium position. A net positive stiffness is provided in closed loop mode with proper

design of the control loop proportional gain. The radial magnetic bearing used in the RMT is an active magnetic bearing manufactured by SEP/S2M. The configuration and development testing of this magnetic bearing were described by Lang (ref. 18). The magnetic bearing is a force actuator and does not support the shaft when operated in open loop mode. When operated in closed loop mode, the magnetic bearing functions as a shaft support element that has significant stiffness and damping capability. Closed loop mode operation is required for some of the test conditions for stability reasons. The closed loop stiffness and damping coefficients of the magnetic bearing vary with frequency as given in Figures 2 and 3. These coefficients were calculated for the frequency range of interest from a transfer function provided by SEP/S2M. The position stiffness, K_y , was calculated to be $-8.76E+6$ N/m ($-50,000$ lb/in) using the nominal air gap and bias current. The maximum force that can be produced by the magnetic bearing with the rotor centered (nominal air gap) is given in Figure 4. Force capacity of the magnetic bearing is based on the maximum current that can be provided to the coils of the bearing. The force capacity is frequency dependent because the coil impedance is frequency dependent. A second constraint on magnetic bearing performance is relative rotor/housing displacement at the magnetic bearing. Maximum displacement at the magnetic bearing is $1.5E-4$ m (6.0 mils) which is one-half of the air gap. The force and displacement constraints are the same for both closed loop and open loop modes.

CONTROL SYSTEM

A block diagram for the magnetic bearing controller is shown in Figure 5. In closed loop mode, the control current is determined by feedback control such that the error between a reference and actual shaft position signal is minimized. This control current is then fed to a current amplifier before going to the electromagnets of the bearing. The magnetic bearing can be used to excite the shaft by using a time varying reference signal.

Two equations that can be written from the block diagram are

$$y_c = y_a - y_o \quad (5)$$

and

$$(F_d - y_c G(s) C_p K_i) / (ms^2 + K_y) = y_a \quad (6)$$

It is necessary to characterize the effect of the reference signal, y_o , on the response of the rotor; therefore, let $F_d = 0$, implying no external disturbing forces such as unbalance.

Substituting Equation (6) into Equation (5) gives

$$(ms^2 + K_y + G(s) C_p K_i) y_a = G(s) C_p K_i y_o \quad (7)$$

From Figure 5, the controlled stiffness of the bearing is

$$F_i / y_c = G(s) C_p K_i \quad (8)$$

This is a complex stiffness that can be represented by (ref. 13)

$$F_i / y_c = K_c + j\omega C \quad (9)$$

where K_c and C are determined by the parameters of the control system, the current stiffness, and the excitation frequency. The position stiffness, K_y , is usually added to the controlled bearing stiffness so that the net stiffness of the magnetic bearing is

$$K = K_c + K_y. \quad (10)$$

The stiffness and damping coefficients given in Figures 2 and 3 are K in Equation 10 and C in Equation 9. Equation 7 may be written in terms of K and C as follows

$$(ms^2 + Cs + K)y_a = (Cs + K - K_y)y_o, \quad (11)$$

using equations 8, 9, and 10 and the substitution $j\omega = s$. If the position reference signal can be represented by

$$y_o = Y_o e^{j\omega t}, \quad (12)$$

then the sinusoidal component of the signal causes a shaft excitation that is similar to the shaft excitation caused by a rotating eccentricity (runout) at a conventional bearing. The position stiffness, K_y , is part of the response to the excitation but not part of the excitation; hence, it is subtracted from the total magnetic bearing stiffness, K , in the excitation term.

The feedback loop is deactivated for open loop mode operation. To excite the shaft in this mode, a control signal is fed directly to the current amplifier, C_p . The force produced is applied directly to the shaft, and no spring exists at the magnetic bearing location except for K_y .

ROTOR DYNAMICS OF THE TESTER

The layout of the tester is shown in Figure 6. The shaft is supported radially by the test article, the radial magnetic bearing, and the slave bearings. In the configuration shown, the test article is a load sharing seal with stiffness variable from $0-1.75E+8$ N/m ($0-1,000,000$ lb/in). The slave bearings form a duplex pair of angular contact ball bearings with stiffnesses of about $1.31E+8$ N/m ($750,000$ lb/in) each as computed by the rolling element computer program of reference 19.

The mode shapes of the first three vibration modes of the tester are shown in Figure 7. A test article stiffness of $8.75E+7$ N/m ($500,000$ lb/in) was used here, but the general character of the mode shapes is the same throughout the stiffness range to be tested. Figure 8 shows the first three forward natural frequencies of the tester as a function of test article stiffness. Results are shown for both closed loop and open loop mode operation of the magnetic bearing. These results are for a rotor speed of $20,000$ cpm; however, the natural frequencies are not strongly dependent on rotor speed. The closed loop stiffness and damping coefficients of the magnetic bearing vary with the vibration mode frequency in accordance with Figures 2 and 3.

Damping for the first two vibration modes varies considerably depending on the test conditions, particularly when testing load sharing seals. Under many of the test conditions, the first two vibration modes of the tester are predicted to be unstable unless the magnetic bearing is used in closed loop mode. Therefore,

closed loop mode operation of the magnetic bearing is required for some of the test conditions.

TEST SIMULATION

The purpose of this analysis is to determine the response at the test article with the magnetic bearing used as an excitation source. Although closed loop mode operation must be used for some of the tests, performance of both operating modes was examined to determine if it would be advantageous to use open loop mode in some instances. In a typical test using the RMT, the rotor is driven at a constant operating speed. The desired test condition is then set for the test article. With closed loop mode operation, the rotor is excited by a frequency sweep of the reference signal, y_0 . With open loop mode operation, the rotor is excited by a frequency sweep of a similar signal applied to the current amplifier of the bearing. Details of this procedure are described by Murphy (ref. 20).

The response of the rotor to closed loop mode excitation can be modelled using

$$[M] \ddot{q} - [G] \dot{\psi} \dot{q} + [K_r] \dot{q} + [C_b] \dot{q} + [K_b] q = ([K_b] - [K_n]) y_0 + [C_b] \dot{y}_0 \quad (13)$$

The matrix, $[K_n]$, has only one nonzero element -- the magnetic bearing position stiffness, K_y , which must be subtracted from the total magnetic bearing stiffness since it is not part of the excitation.

The excitation is represented by

$$y_0 = Y_0 e^{j\omega t}$$

and the response by

$$q = Q e^{j(\omega t + \phi)}.$$

As described above, the excitation signal (reference signal) forces the rotor in the same way as a rotating eccentricity at a conventional bearing. To simulate a test, the excitation is applied at the magnetic bearing degree-of-freedom to represent the dynamic reference signal, y_0 , fed to the control system. The rotor spin speed, ψ , is held constant at the desired testing speed and all bearing elements other than the magnetic bearing are given constant values based on the constant rotor speed. Equation 13 is solved for various values of the excitation frequency, ω , to obtain the response of the rotor over the frequency range of interest.

Figures 9 - 12 show predicted results for a constant rotor speed of 20,000 cpm and a test article stiffness of $1.75E+7$ N/m (100,000 lb/in). Figure 9 shows a comparison of predicted transfer function amplitudes at the test article for closed and open loop operation. The transfer function for the closed loop curve is calculated based on the excitation force produced by y_0 . The transfer function for the open loop curve is calculated based on the forcing function applied at the magnetic bearing. The response of the first vibration mode is much lower with closed loop operation due to the higher damping.

In Figures 10-12, three constraints are placed on the system that determine the maximum response at the test article: 1) the magnetic bearing applied force, F_i ,

cannot exceed the values given in Figure 4, 2) displacement at the magnetic bearing cannot exceed $1.5E-4$ m (6.0 mils), and 3) based on clearance, the maximum allowable displacement at the test article is $1.0E-4$ m (4.0 mils). The net force provided by the magnetic bearing in closed loop mode includes both the excitation force from y_0 and the reaction force due to the measured rotor motion. The force produced by the position stiffness, K_y , is not included in the constraint. The input signal varies with frequency as necessary to produce the maximum response at each frequency.

These three physical constraints serve to place an upper limit on tester response to magnetic bearing excitation. In addition, there are also two minimum conditions which must be satisfied. The two primary measured quantities of test article displacement and load must be large enough to be accurately measured with the given instrumentation. The lower limits are $1.25E-5$ m (0.5 mils) of test article displacement and $1.5E-6$ m (50 μ in) of flex mount deflection. An appreciable range between the upper and lower operating limits is desirable so that tests on amplitude linearity could be performed.

Figure 10 is a comparison of the maximum response at the test article for closed and open loop modes. The response exceeds the requirement of $1.25E-5$ m (0.5 mils) throughout the frequency range for both control modes. There appears to be only one curve in the figure because the responses are the same for the two control modes. The reason the curves are the same is that either of the first two constraints (force and displacement at the magnetic bearing) applied in the analysis serves to prescribe the rotor motion at the magnetic bearing regardless of the magnetic bearing stiffness and damping. The third constraint prescribes the motion at the test article. Since all of the constraints are the same for both control modes, the test article responses are identical.

Figure 11 shows the maximum displacement of the flex mount load sensing element. The curve is similar to that of Figure 10, and shows that the required displacement of $1.25E-6$ m (50 μ in) is achieved over most of the frequency range, regardless of control mode.

Figures 12 - 14 show predicted results for a constant rotor speed of 20,000 cpm and a test article stiffness of $1.3E+8$ N/m (750,000 lb/in). Figure 12 shows a comparison of the predicted closed and open loop transfer function amplitudes at the test article. Again, response is lower with closed loop mode operation due to higher damping. A comparison of Figures 12 and 9 shows that test article response for a given force at the magnetic bearing is lower with the higher test article stiffness.

Figure 13 shows a comparison of the maximum response at the test article for closed and open loop modes. Again, the response is nearly the same for the two control modes, and the requirement of $1.25E-5$ m (0.5 mils) displacement is met throughout most of the frequency range. A comparison of Figures 13 and 10 shows that the response at the test article is lower when the test article stiffness is higher.

Figure 14 shows the maximum displacement of the flex mount load sensing element. The required displacement of $1.25E-6$ m (50 μ in) is again achieved over most of the frequency range, regardless of control mode. By comparison of Figures 11 and 14, flex mount deflection is much higher with the higher test article stiffness.

Figures 10 and 13 show that the maximum response at the test article is the same for both open loop and closed loop modes. This result is due to the nature of the constraints that are placed on the analysis to determine the maximum response. This analysis does not consider the effect of synchronous loading due to unbalance. A given unbalance loading would cause a displacement response at the test article and at the magnetic bearing that would subtract directly from the allowable displacement at either location. The responses would be different for closed and open loop modes because the shaft eigenvalues are different in the two control modes. Also, a given unbalance loading would cause a reaction force at the magnetic bearing when the magnetic bearing is operated in closed loop mode. This reaction force would reduce the allowable magnetic bearing force available to excite the rotor. The net effect of unbalance is to lower the maximum achievable test article response in either control mode. This reduction in maximum test article response is minimized by operating the tester at spin speeds that are adequately distant from the rotor natural frequencies. Based on the maximum expected unbalance levels for the RMT, response due to unbalance should not exceed $1.0E-5$ m (0.4 mils) at either the test article or the magnetic bearing for any of the planned test conditions with either operating mode. The closed loop reaction force at the magnetic bearing for the maximum expected unbalance force is about 330N (75 lbs), or less than 10% of the dynamic load capacity of the magnetic bearing. Therefore, the desired test article response levels should still be achieved.

CONCLUSIONS

An analysis was presented here that shows closed loop mode excitation of a rotor by a magnetic bearing to be analogous to the excitation produced by a rotating eccentricity at a conventional bearing. Open loop mode excitation can be treated simply by applying a forcing function directly to the shaft. These two methods were used to predict the maximum response of the Rocketdyne Multifunction Tester to magnetic bearing excitation in either control mode. The results show that the required response levels at the test article location are achievable over most of the frequency range. The analysis also predicts that maximum response will be the same for both open and closed loop modes. This result was due to the nature of the constraints that were used to determine maximum response. The analysis does not consider the effect of residual unbalance in the tester rotor. A synchronous unbalance loading would reduce, by differing amounts, the maximum test article response achievable in either control mode. Based on expected unbalance levels, the desired test article response levels should still be achieved.

NOMENCLATURE

| | | |
|---------|---|--|
| A_p | = | cross section area of one pole of a magnetic bearing |
| C | = | magnetic bearing damping |
| $[C_b]$ | = | bearing damping matrix |
| C_p | = | current amplifier gain |
| e | = | base of the natural logarithm |
| F | = | magnetic force in an air gap |
| F_d | = | any disturbance force, such as unbalance |
| F_j | = | net controlled force applied by magnetic bearing |
| $[G]$ | = | rotor gyroscopic matrix |
| $G(s)$ | = | controller closed loop transfer function |
| h | = | magnetic bearing air gap thickness |
| h_s | = | nominal magnetic bearing air gap thickness |

| | | |
|----------|---|---|
| i | = | current in magnetic bearing coil |
| i_c | = | control current |
| i_s | = | steady or bias current in magnetic bearing coil |
| j | = | square root of -1 |
| K | = | net magnetic bearing stiffness |
| $[K_b]$ | = | bearing stiffness matrix |
| K_c | = | magnetic bearing controlled stiffness |
| K_i | = | magnetic bearing current stiffness |
| $[K_n]$ | = | magnetic bearing position stiffness matrix |
| $[K_r]$ | = | rotor free/free stiffness matrix |
| K_y | = | magnetic bearing position stiffness |
| m | = | effective mass of the rotor |
| $[M]$ | = | rotor mass matrix |
| N | = | number of turns in magnetic bearing coil |
| q | = | physical displacement vector |
| s | = | Laplace variable |
| t | = | time |
| y | = | vertical position |
| y_a | = | actual (measured) rotor position |
| y_c | = | error signal |
| y_o | = | position reference signal |
| ϕ | = | phase angle |
| ψ | = | rotor spin speed |
| μ | = | magnetic permeability |
| μ_0 | = | magnetic permeability of free space |
| ω | = | excitation frequency |

REFERENCES

1. Schweitzer, G. and Lange, R., "Characteristics of a Magnetic Rotor Bearing for Active Vibration Control," "First International Conference on Vibration in Rotating Machinery, I. Mech. Eng., Cambridge, September 1976, Paper No. C239/76.
2. Stanway, R. and Burrows, C.R., "Active Vibration Control of a Flexible Rotor on Flexibly-Mounted Journal Bearings," ASME J. Dynamic Systems, Measurement, and Control, Vol. 103, 1981, pp. 383-388.
3. Salm, J. and Schweitzer, G., "Modelling and Control of a Flexible Rotor with Magnetic Bearings," Third International Conference on Vibrations in Rotating Machinery, I. Mech. Eng., Cambridge, September 1984, Paper No. C277/84.
4. Nikolajsen, J.L., Holmes, R., and Gondhalekar, V., "Investigation of an Electromagnetic Damper for Vibration Control of a Transmission Shaft," Proc. Instn. Mech. Engrs., Vol. 193, 1979, pp. 331-336.
5. Allaire, P.E., Lewis, D.W., and Knight, J.D., "Active Vibration Control of a Single Mass Rotor on Flexible Supports," J. Franklin Inst., Vol 315, 1983, pp. 211-222.
6. Kasarda, M.E.F., Allaire, P.E., Humphris, R.R., and Barrett, L.E., "A Magnetic Damper for First Mode Vibration Reduction in Multimass Flexible Rotors," Gas Turbine and Aeroengine Congress and Exposition, Toronto, June 1989, ASME Paper 89-GT-213.

7. Foster, E.G., Kulle, V. and Peterson, R.A., "The Application of Active Magnetic Bearings to a Natural Gas Pipeline Compressor," ASME Paper 86-GT-61, 1986.
8. Weise, D.A., "Present Industrial Applications of Active Magnetic Bearings," 22nd Intersociety Energy Conversion Engineering Conference, Philadelphia, August 1987.
9. Brunet, M., "Practical Applications of the Active Magnetic Bearings to the Industrial World," Proc. of First International Symposium on Magnetic Bearings, Zurich, June 1988, pp. 225-244.
10. Habermann, H. and Brunet, M., "The Active Magnetic Bearing Enables Optimum Damping of Flexible Rotor," ASME Paper 84-GT-117, 1984.
11. Weise, D.A., "Active Magnetic Bearings Provide Closed Loop Servo Control for Enhanced Dynamic Response," 27th IEEE Machine Tool Conference, October 1985.
12. Humphris, R.R., Kelm, R.D., Lewis, D.W., and Allaire, P.E., "Effect of Control Algorithms on Magnetic Journal Bearing Properties," Journal of Engineering for Gas Turbines and Power, Vol. 108, No. 4, 1986, pp. 624-632.
13. Chen, H.M. and Darlow, M.S., "Design of Active Magnetic Bearings with Velocity Observer," ASME 11th Biennial Conference on Mechanical Vibration and Noise, Boston, September 1987.
14. Chen, H.M., "Magnetic Bearings and Flexible Rotor Dynamics," STLE Paper 88-AM-2D-1, 1988.
15. Sutton, R.F., "LOX/Hydrocarbon Turbomachinery Technology," JANNAF Propulsion Meeting, San Diego, 1987.
16. Ulbrich, H., "New Test Techniques Using Magnetic Bearings," Proc. of First International Symposium on Magnetic Bearings, Zurich, June 1988, pp. 281-288.
17. Wagner, N.G., and Pietruszka, W.D., "Identification of Rotordynamic Parameters on a Test Stand with Active Magnetic Bearings," Proc. of First International Symposium on Magnetic Bearings, Zurich, June 1988, pp. 289-299.
18. Lang, K.W., "Test of an Active Magnetic Bearing in Liquid Nitrogen," 12th Biennial Conference on Mechanical Vibration and Noise, Montreal, ASME Pub. DE-Vol. 18-1, 1989, pp. 321-326.
19. Jones, A.B., "A General Theory for Elastically Constrained Ball and Radial Roller Bearings Under Arbitrary Load and Speed Conditions," ASME Journal of Basic Engineering, Vol. 82, 1969, p. 309.
20. Murphy, B.T., Scharrer, J.K., and Sutton, R.F., "The Rocketdyne Multifunction Tester, Part I - Test Method," Rotor Dynamics Instability Problems in High Performance Turbomachinery, Texas A&M University, May 1990.

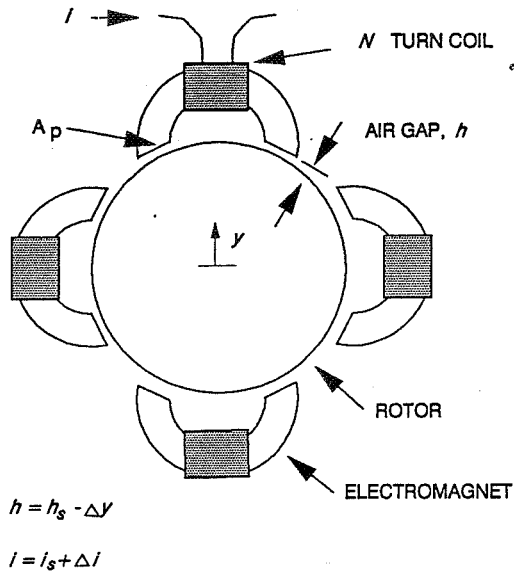


Figure 1. Magnetic Bearing Schematic

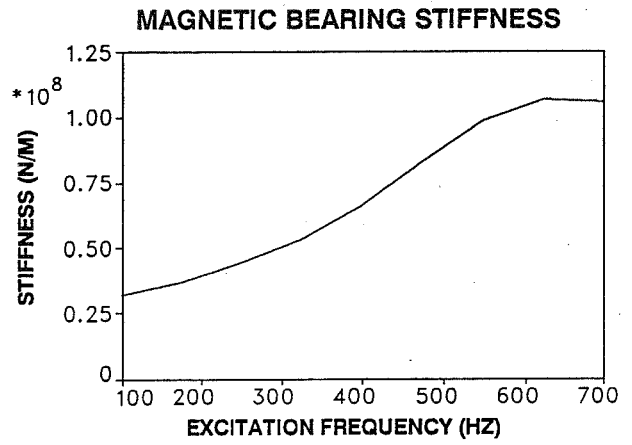


Figure 2. Magnetic Bearing Stiffness Coefficient vs. Excitation Frequency

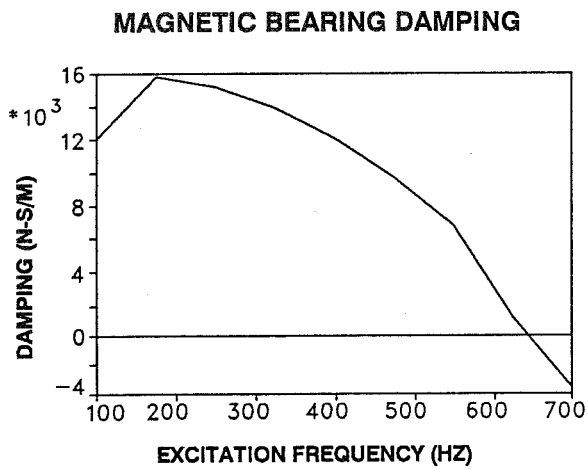


Figure 3. Magnetic Bearing Damping Coefficient vs. Excitation Frequency

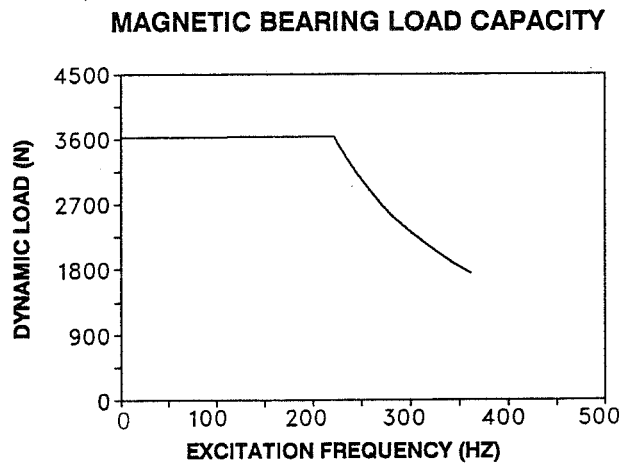


Figure 4. Magnetic Bearing Load Capacity vs. Excitation Frequency

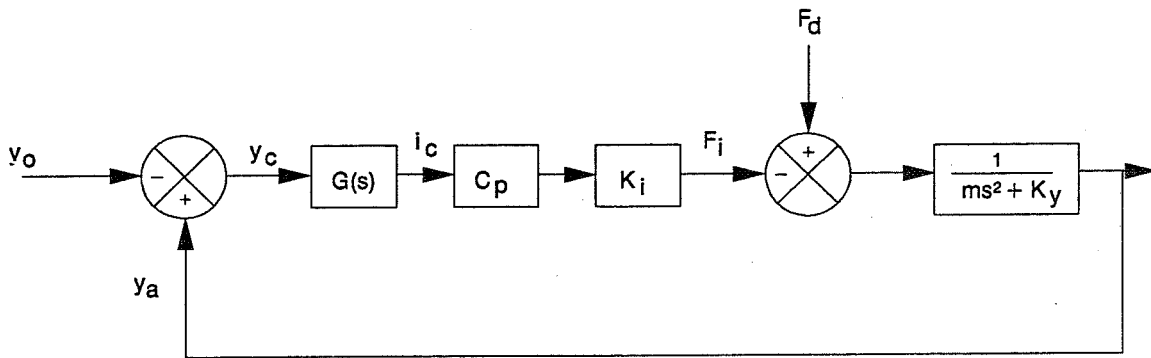


Figure 5. Magnetic Bearing Control Diagram

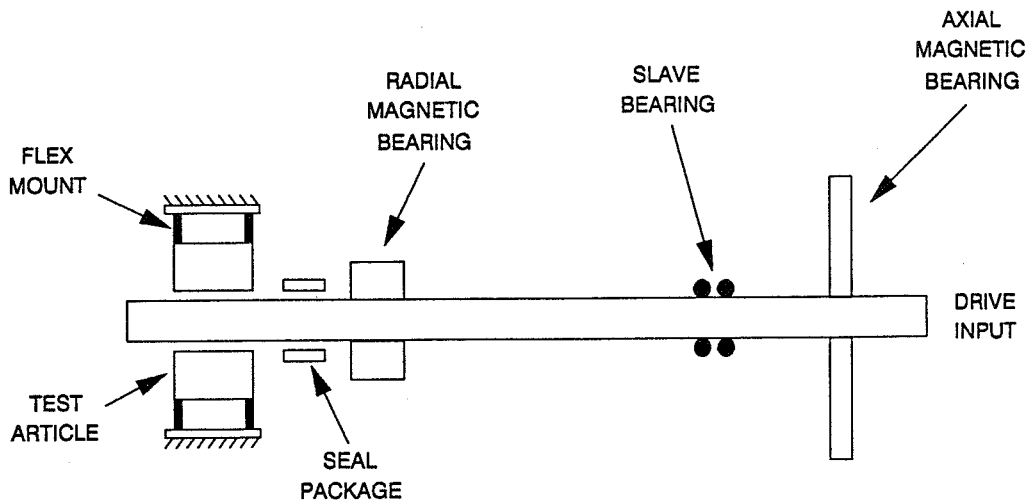


Figure 6. Schematic of Rocketdyne Multifunction Tester

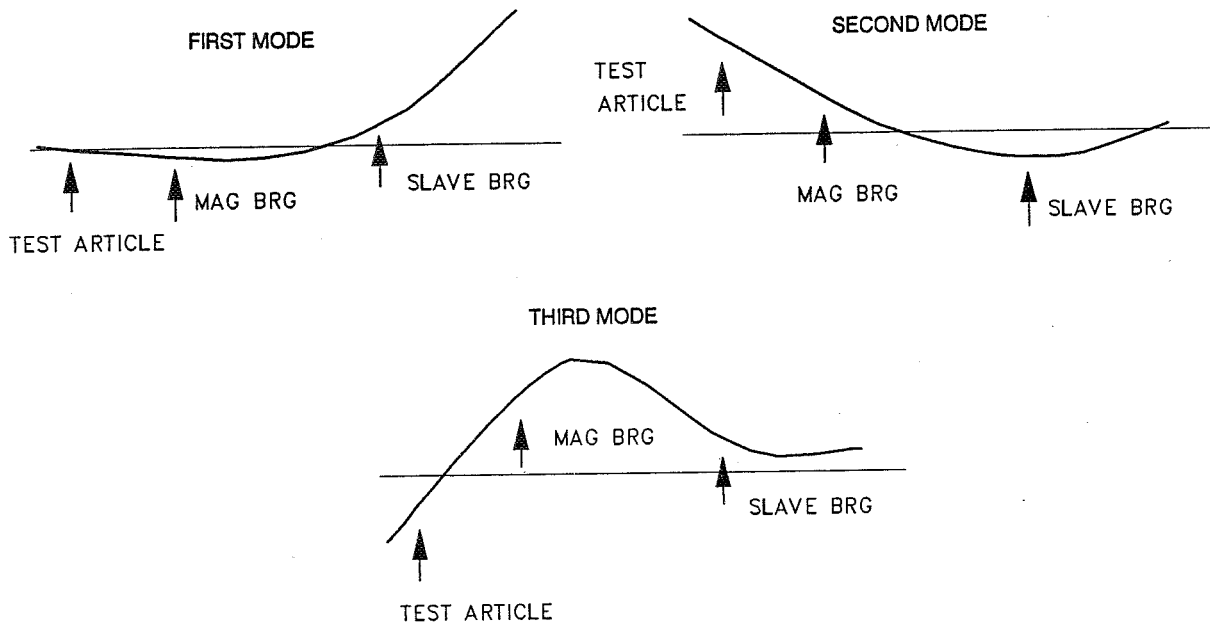


Figure 7. Mode Shapes for the First Three Vibration Modes of the Tester

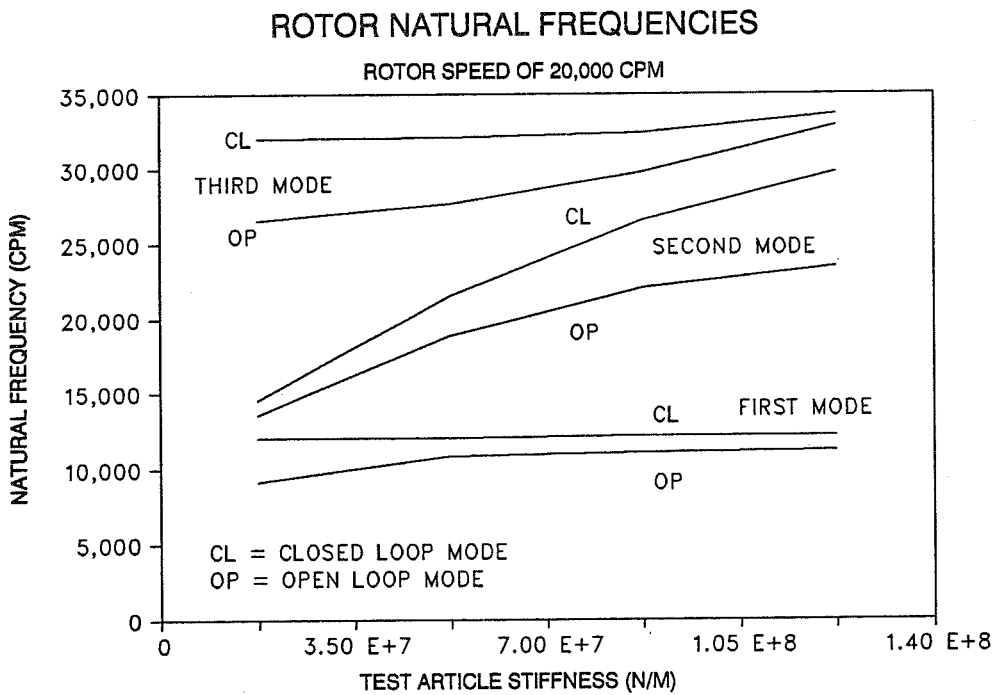


Figure 8. Natural Frequencies vs. Test Article Stiffness for Tester

TEST ARTICLE TRANSFER FUNCTION

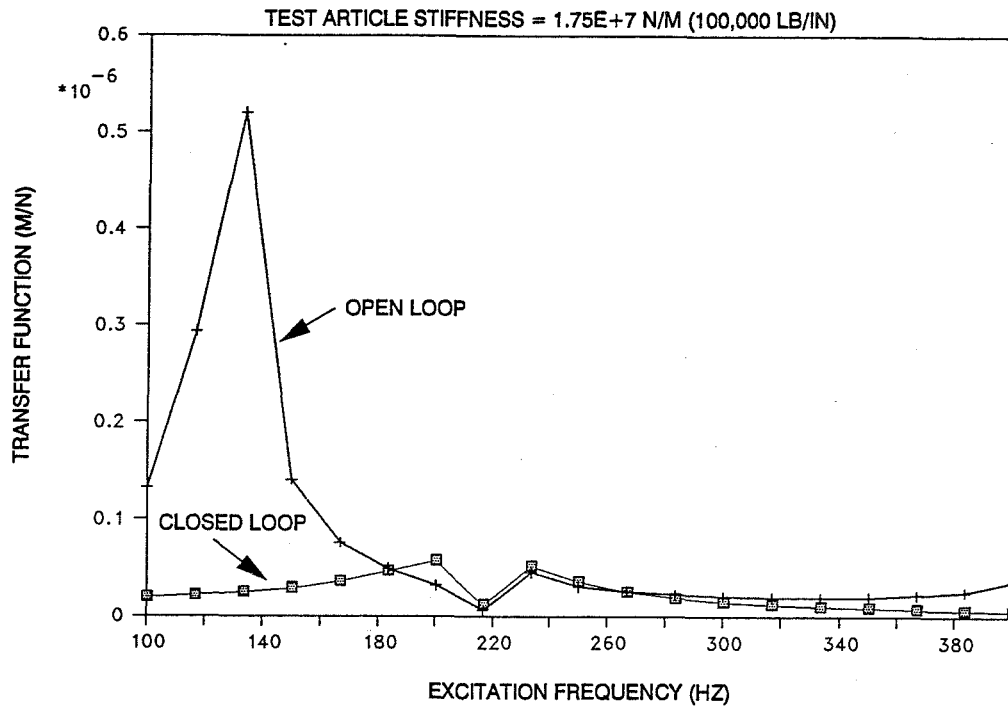


Figure 9. Transfer Function Amplitude, Response at Test Article due to Force at Magnetic Bearing, Test Article Stiffness = 100,000 lb/in.

MAXIMUM TEST ARTICLE RESPONSE

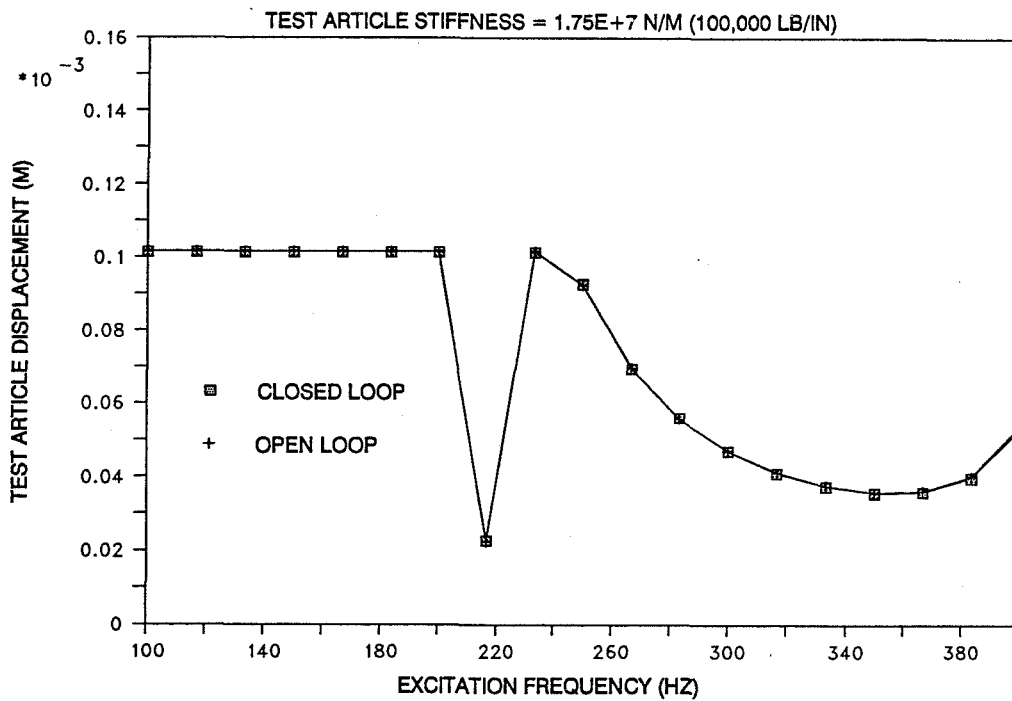


Figure 10. Maximum Response at Test Article, Test Article Stiffness = 100,000 lb/in.

MAXIMUM FLEX MOUNT RESPONSE

TEST ARTICLE STIFFNESS = $1.75E+7$ N/M (100,000 LB/IN)

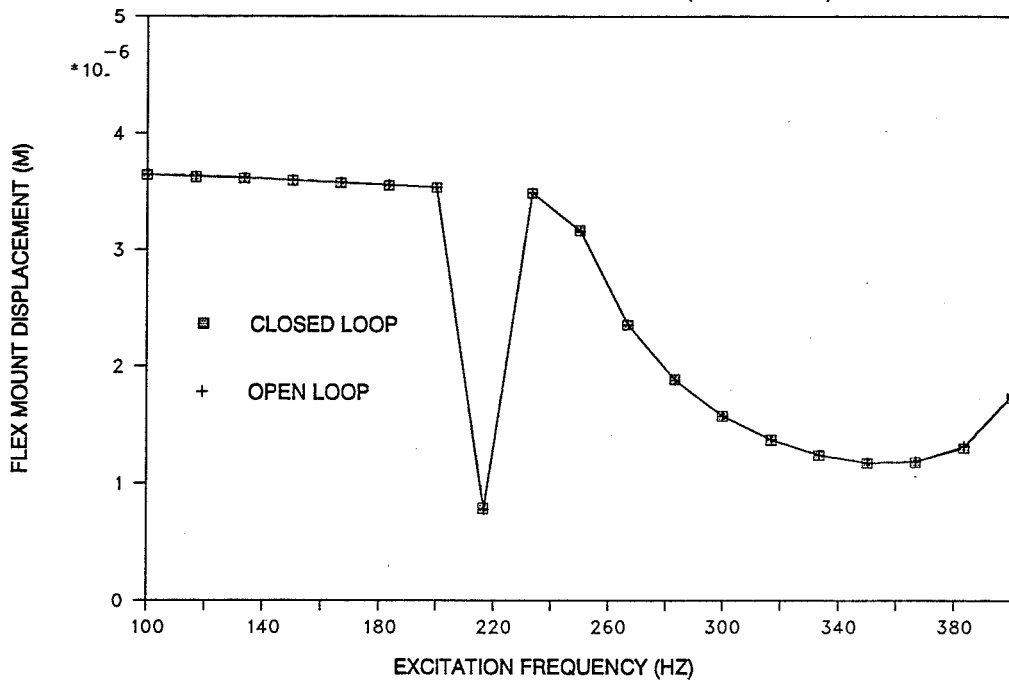


Figure 11. Maximum Response at Flex Mount Load Sensing Element, Test Article Stiffness = 100,000 lb/in.

TEST ARTICLE TRANSFER FUNCTION

TEST ARTICLE STIFFNESS = $1.31E+8$ N/M (750,000 LB/IN)

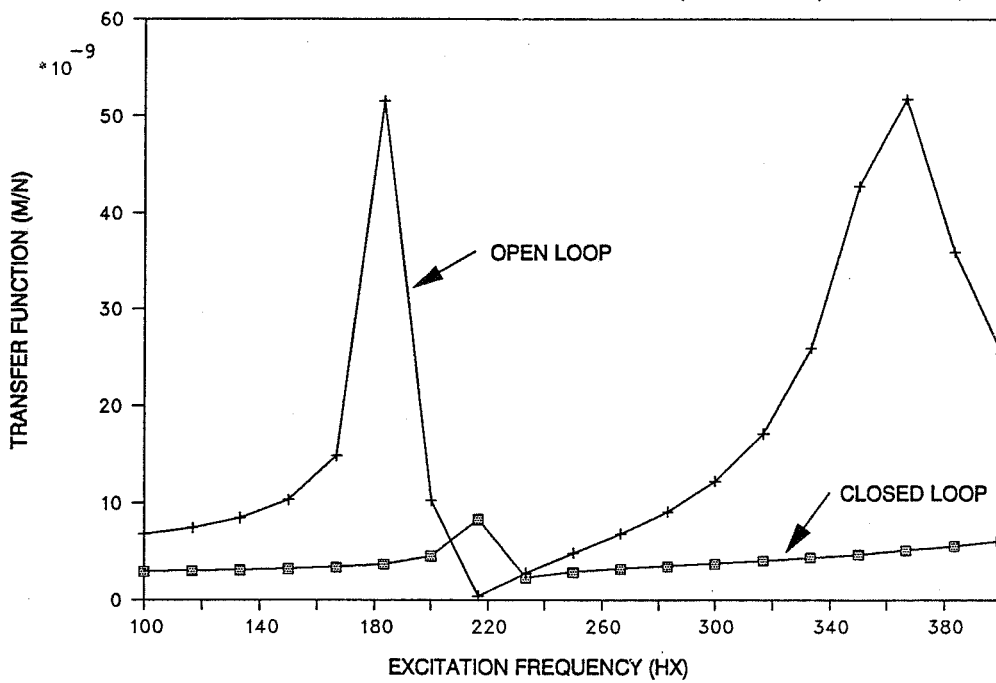


Figure 12. Transfer Function Amplitude, Response of Test Article due to Force at Magnetic Bearing, Test Article Stiffness = 750,000 lb/in

MAXIMUM TEST ARTICLE RESPONSE

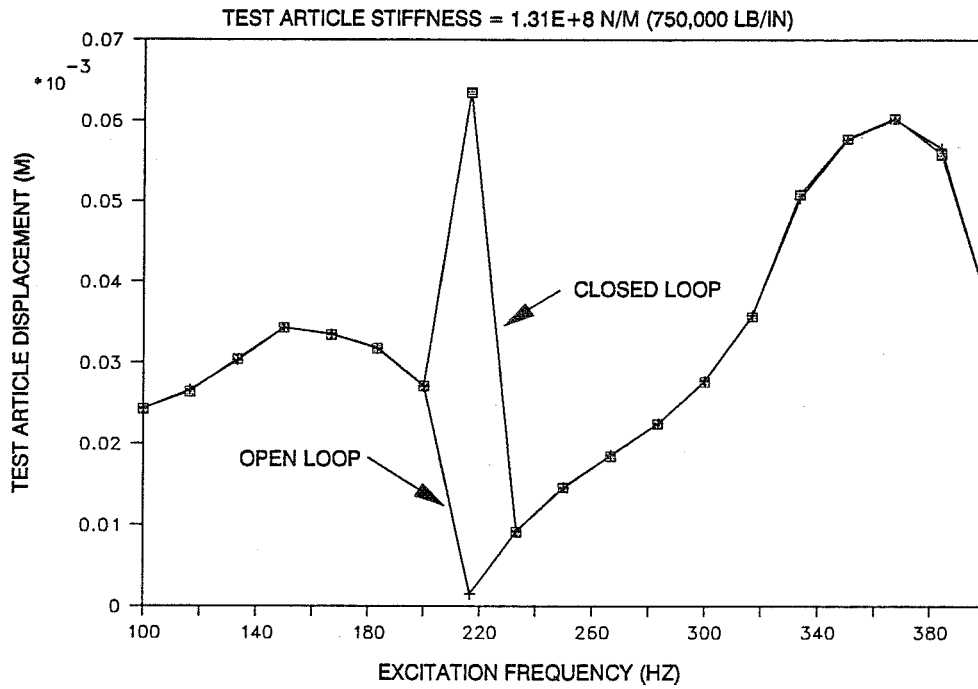


Figure 13. Maximum Response at Test Article,
Test Article Stiffness = 750,000 lb/in.

MAXIMUM FLEX MOUNT RESPONSE

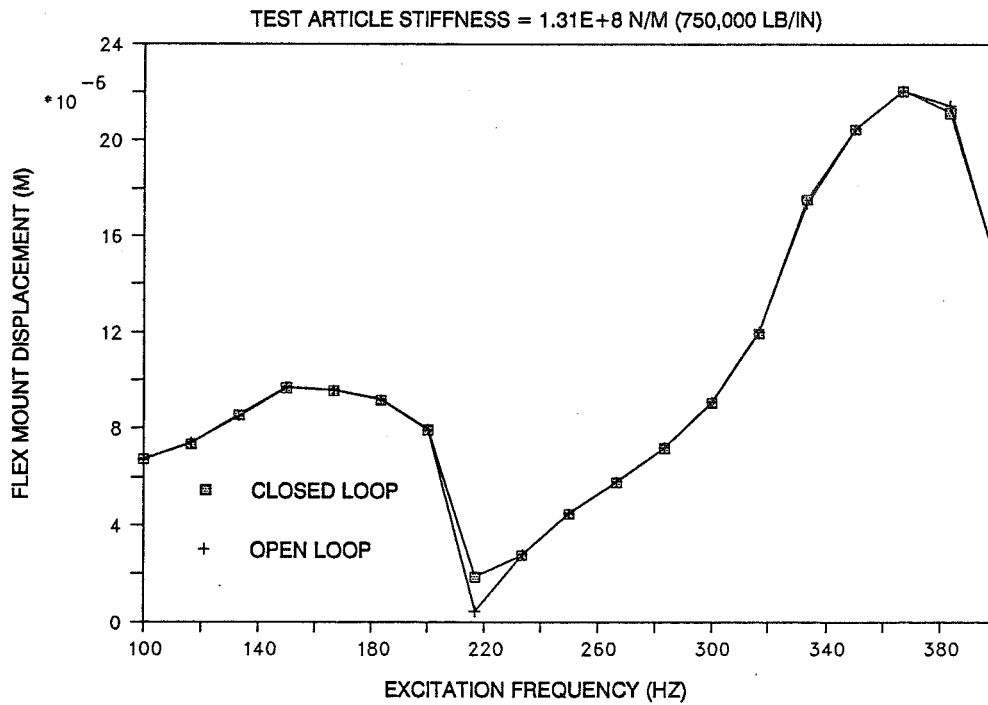


Figure 14. Maximum Response at Flex Mount Load Sensing Element,
Test Article Stiffness = 750,000 lb/in.